

DESIGN AND THERMAL PERFORMANCE ANALYSIS OF A NEW WATER-COOLED STRUCTURE FOR PERMANENT MAGNET SYNCHRONOUS MOTORS FOR ELECTRIC VEHICLES

by

Jiacheng ZHANG* and Baojun GE

National Engineering Research Center of Large Electric Machines and Heat Transfer Technology
School of Electrical and Electronic Engineering, Harbin University of Science and Technology,
Harbin, China

Original scientific paper
<https://doi.org/10.2298/TSCI220613153Z>

In order to solve the problem of severe stator winding heating due to the single cooling structure of a permanent magnet synchronous motor for electric vehicles, and to further improve the heat transfer capability of the permanent magnet synchronous motor, a new water-cooled structure is proposed in which cooling pipes are placed at the stator yoke to increase the heat transfer area. In order to evaluate the heat transfer effect of this new water-cooled structure, this paper takes a 50 kW permanent magnet synchronous motor for electric vehicles as the research object. By establishing a 3-D full-domain fluid-solid coupled heat transfer model, setting boundary conditions and reasonable assumptions, the full-domain fluid-heat coupled field of the permanent magnet synchronous motors is calculated numerically, and the fluid-flow characteristics and heat transfer variation laws of the new water-cooled structure are analyzed. The results show that compared with the original cooling structure, the maximum temperature drop of stator winding and permanent magnet can reach 5.23% and 11.17%, respectively. The results obtained can provide a reference for future research on the thermal performance and water-cooled structure optimization of permanent magnet synchronous motor for electric vehicles.

Key words: *permanent magnet synchronous motor, water-cooled structure, heat transfer capability, numerical simulation*

Introduction

Compared with traditional induction motors, permanent magnet synchronous motors (PMSM) have been widely used as the core drive mechanism of electric vehicles (EV) due to their high power density, fast response speed, and wide speed regulation range. In addition, the PMSM for vehicles also has a sufficiently competitive output power to meet the power requirements of the EV. Therefore, the PMSM for EV often matches the design of high intensity electromagnetic load. However, during the driving process of the EV, the thermal load of the PMSM increases with the increase of the current density of the stator winding, and considering the single water-cooled structure and the thicker insulation bound at the end of the stator winding, the aforementioned factors will together make it difficult to transfer heat from the stator winding. The high temperature of PMSM for EV will increase the risk of abnormal aging of stator winding insulation [1] and the risk of irreversible demagnetization of permanent magnets [2, 3]. In severe cases, it will endanger the entire drive system and directly affect the driving

* Corresponding author, e-mail: qingjide@foxmail.com

safety and reliability of EV. Therefore, in order to guarantee the safety and stability of PMSM at high stator winding currents and high thermal loads, it is particularly important to design effective water-cooled structure and to analyze and calculate its precise heat transfer characteristics.

There is more than one method for calculating heat transfer in PMSM, such as the finite element method [4-7], the thermal network method [8-10], and the finite volume method [11]. In order to investigate the relationship between electromagnetic losses and heat losses in high power switched reluctance motors (SRM), Yan *et al.* [12] introduced electromagnetic losses in the form of internal heat production of motor components into the thermal analysis model, thus revealing the variation pattern between heat losses and electromagnetic losses in high power SRM under air-cooled, water-cooled and hybrid cooling systems. Zhang *et al.* [13] combined electromagnetic finite element analysis with thermal resistance networks to conduct a comparative study of the electromagnetic and thermal performance of PMSM under different working conditions, and demonstrated the advantages of the improved coupled analysis method in terms of computational efficiency and accuracy. On the basis of accurate calculation of the heat transfer characteristics of PMSM, it is also necessary to design a reasonable and effective motor heat transfer structure in order to ensure reliable operation of PMSM [14-19]. Fan *et al.* [20] proposed a new water-cooled topology for the thermal management of PMSM with centralized windings and evaluated the thermal performance of such a new water-cooled topology using the finite element method. The evaluation results showed that the winding temperature could be reduced by more than 20 °C using this cooling structure. Acquaviva *et al.* [21] used thermally conductive epoxy resin to create heat transfer channels in the stator slots, proposed a heat transfer scheme with direct oil cooling in the stator slots, and combined with finite element analysis to perform conjugate heat transfer simulations of the motor to obtain the effect of the cooling fluid on the stator winding temperature rise at different flow rates. Although positive progress has been made in the optimization of the cooling structure of PMSM for EV, the singularity of the cooling structure still limits further improvements in the electromagnetic and thermal capabilities of the motor.

In order to further improve the heat transfer capability of the PMSM and to solve the problem of severe stator winding heating, this study sets the cooling pipes at the stator yoke as a new water-cooled structure. In order to increase the heat transfer area, 24 cooling pipes were placed at the lower magnetic density of the motor yoke. The aim of this study is to describe the cooling performance of this new water-cooled structure for PMSM for EV. By comparing the original cooling structure, a 3-D fluid-solid coupled heat transfer model of a PMSM including the stator winding ends is established, the flow pattern and variation law of the cooling fluid inside the cooling pipes are investigated by using the finite element method, and the effect of the use of cooling pipes on the heat transfer capability of the motor is analyzed for a wide range of temperatures and flow rates of the cooling fluid inside the water jacket. The simulation results show that the new water-cooled structure proposed in this paper can effectively improve the heat transfer capability of PMSM.

Modelling and boundary conditions of PMSM

Mathematical models establishment

The physical laws that govern the flow and heat transfer of cooling fluids within the motor are the basis for establishing the basic set of equations of fluid motion. These laws include the three laws of conservation of mass, conservation of momentum and conservation of energy.

To control fluid-flow in the fluid-solid coupled heat transfer model, the mass conservation is given:

$$\frac{\partial \rho}{\partial t} + \frac{\partial(\rho \mathbf{u})}{\partial x} + \frac{\partial(\rho \mathbf{v})}{\partial y} + \frac{\partial(\rho \mathbf{w})}{\partial z} = 0 \quad (1)$$

where ρ is the fluid density, t – the time, \mathbf{u} , \mathbf{v} , and \mathbf{w} are the fluid velocity.

The flow of cooling fluid in the water jacket and cooling pipes shall also conform to the law of conservation of momentum, which is given:

$$\begin{aligned} \frac{\partial(\rho \mathbf{u})}{\partial t} + \text{div}(\rho \mathbf{u} \mathbf{u}) &= -\frac{\partial p}{\partial x} + \frac{\partial \tau_{xx}}{\partial x} + \frac{\partial \tau_{yx}}{\partial y} + \frac{\partial \tau_{zx}}{\partial z} + F_x \\ \frac{\partial(\rho \mathbf{v})}{\partial t} + \text{div}(\rho \mathbf{v} \mathbf{u}) &= -\frac{\partial p}{\partial y} + \frac{\partial \tau_{xy}}{\partial x} + \frac{\partial \tau_{yy}}{\partial y} + \frac{\partial \tau_{zy}}{\partial z} + F_y \\ \frac{\partial(\rho \mathbf{w})}{\partial t} + \text{div}(\rho \mathbf{w} \mathbf{u}) &= -\frac{\partial p}{\partial z} + \frac{\partial \tau_{xz}}{\partial x} + \frac{\partial \tau_{yz}}{\partial y} + \frac{\partial \tau_{zz}}{\partial z} + F_z \end{aligned} \quad (2)$$

where i is the co-ordinate direction, F_i – the volume force on the microelement, p – the static pressure on the fluid microelement, and τ_{xx} , τ_{xy} and τ_{xz} are the viscous stress components on the surface of the microelement.

The heat transfer process during motor operation shall comply with the law of conservation of energy, which is described:

$$\frac{\partial(\rho T)}{\partial t} + \text{div}(\rho \mathbf{u} T) = \text{div} \left(\frac{k}{c_p} \text{grad} T \right) + S_T \quad (3)$$

where c_p is the specific heat capacity, T – the temperature of the fluid, k is the heat transfer coefficient of the fluid, and S_T – the fluid heat source.

The basic principles of fluid mechanics and heat transfer show that the flow and heat transfer of the cooling fluid in a PMSM for EV satisfy the laws of conservation of mass, momentum and energy, and the k - ε turbulence model is the most widely used in the field of fluid calculation in the cooling pipes at present. In addition fully considering the axial and radial flow of fluid in the cooling pipes, the model also adds an additional term to the turbulent dissipation rate equation, which helps to improve the accuracy of the flow field with large velocity gradient, so the turbulent fluid is described by the k - ε turbulence model and the RNG control equations, they are described:

$$\frac{\partial}{\partial t}(\rho k) + \text{div}(\rho k \mathbf{V}) = \text{div} \left[\left(\mu + \frac{\mu_t}{\sigma_k} \right) \text{grad} k \right] + G_k - \rho \varepsilon \quad (4)$$

$$\frac{\partial}{\partial t}(\rho \varepsilon) + \text{div}(\rho \varepsilon \mathbf{V}) = \text{div} \left[\left(\mu + \frac{\mu_t}{\sigma_\varepsilon} \right) \text{grad} \varepsilon \right] + C_{1\varepsilon} \frac{\varepsilon}{k} G_k - C_{2\varepsilon} \rho \frac{\varepsilon^2}{k} \quad (5)$$

where k is the feature speed of turbulence kinetic energy, \mathbf{V} – the fluid velocity vector, ε – the diffusion factor, α_k and α_ε are the reciprocals of the prandtl number of equations k and ε , respectively, μ_t – the eddy viscosity coefficient, G_k – the turbulence generation rate, and $C_{1\varepsilon}$ and $C_{2\varepsilon}$ are the constants.

Physical model establishment

The PMSM for EV studied in this paper is shown in fig. 1. As can be seen in fig. 1, the motor has a spiral water jacket inside the casing, and if this single water-cooled structure (spiral water jacket) is used, the motor's heat transfer capability will not be enhanced. In order to improve the heat transfer capability of the PMSM, additional cooling pipes are provided in the stator yoke.

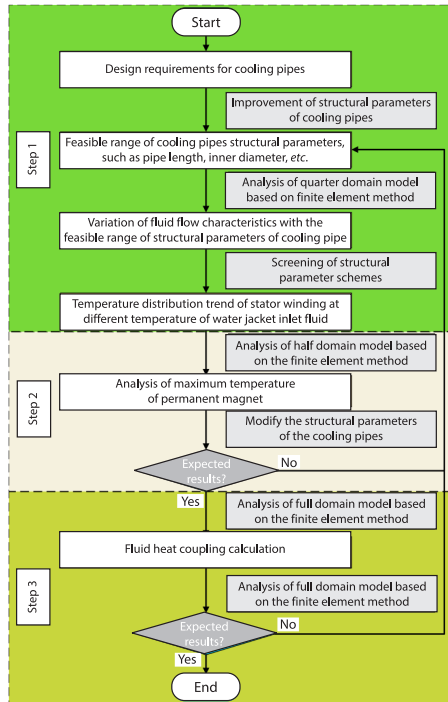


Figure 1. Design process of cooling pipe

The design process of cooling pipe is shown in fig. 1. For clarity in the following, the inner and outer sides of the cooling pipe bend are marked in fig. 2.

The main basic parameters of the motor are given in tab. 1. The insulation class of the PMSM studied in this paper is class F. This represents a limit working temperature that is 155 °C for the stator windings and permanent magnets, but for the stability and safety of the motor, the working temperatures of the stator windings and permanent magnets generally do not exceed 120 °C and 155 °C.

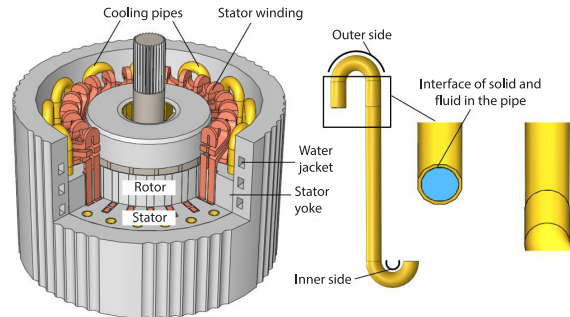


Figure 2. Physical model of the PMSM with a new water-cooled structure

Table 1. Basic parameters of the PMSM and the cooling pipe

Parameter	Value	Parameter	Value
Number of stator slots	24	Number of phases	3
Number of poles	8	Rated power [kW]	50
Outer diameter of stator [mm]	250	Insulation class	F
Material of cooling pipe	Aluminum alloy	Inner diameter of cooling pipe [mm]	8
Quantity of cooling pipe	24	Average Reynolds number in the cooling pipe	14400

Figure 3 shows the hexahedral mesh of the PMSM based on the poly-hexcore method. Compared to the meshes generated by other methods, the mesh generated by the poly-hexcore method has the advantages of high orthogonal quality and low mesh distortion. This method enables the mesh generation of complex fluid-solid coupling models, thus ensuring convergence and accuracy in the numerical calculation of PMSM. The number of meshes for the fluid-solid coupling model of the PMSM for EV studied in this paper is 8.92 million, among them, the number of grids in the cooling pipes calculation domain is 0.83 million. Next, the independence of the grid is verified by calculating the change of turbulent kinetic energy of the fluid in the pipes with different grid numbers. Figure 4 shows the variation of the average turbulent kinetic energy with time under different grid numbers. When the number of grids is less than 0.83 million, the decay rate of turbulent kinetic energy of the fluid in the pipes accelerates, but with the increase of the number of grids, the turbulent kinetic energy in the cooling pipes tends to

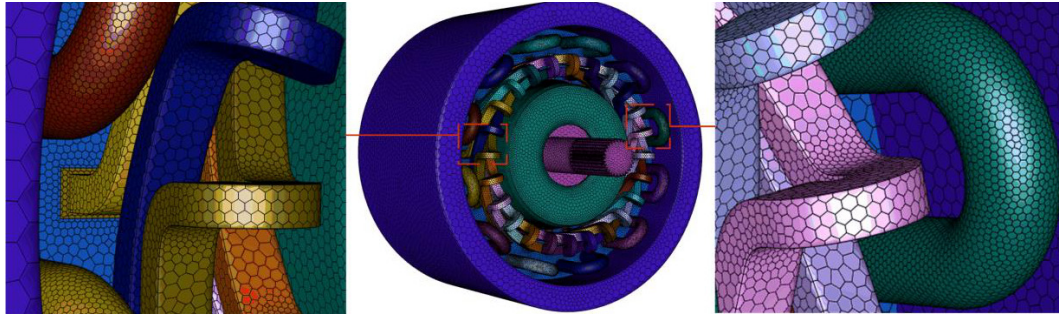


Figure 3. Hexahedral mesh for PMSM based on poly-hexcore method

stabilize in the simulation process. The results show that the decay rate of turbulent kinetic energy is almost the same between the number of 0.83 million grids and 0.97 million grids. Considering the calculation accuracy and efficiency, the number of grids in the cooling pipes calculation domain is 0.83 million in the next simulation calculation.

Basic assumptions

- The fluid-flow velocity inside the PMSM is much less than the speed of sound, so the fluid is treated as an incompressible viscous fluid.
- Given the large Reynolds number of the fluid in the motor, the turbulence model is used to solve for the fluid field.
- The effect of buoyancy and gravity on the fluid in the motor is not taken into account.
- The contact thermal resistance between the core stacks is neglected and all parts of the motor are considered to be well insulated.

Boundary conditions

According to the stable working performance of the PMSM at rated operation and combined with the characteristics of the motor cooling structure, the following boundary conditions are given:

- The water temperature and flow rate at the inlet of the cooling pipe were kept constant at 40 °C and 1.2 m/s, respectively, while the initial values of water temperature and flow rate at the inlet of the spiral water jacket were 40 °C and 1.12 m/s, respectively, which subsequently changed as the simulation progressed.
- The inlet of spiral water jacket is defined as velocity inlet, and the boundary conditions of cooling pipes outlet and spiral water jacket outlet are consistent.
- The outer wall surface of the rotor is set as a rotating wall surface according to the actual working conditions of the PMSM.

Results and discussion

Figure 5 shows the effect of the use of cooling pipes on the maximum temperature of the stator winding and permanent magnet for a wide range of temperatures for the cooling

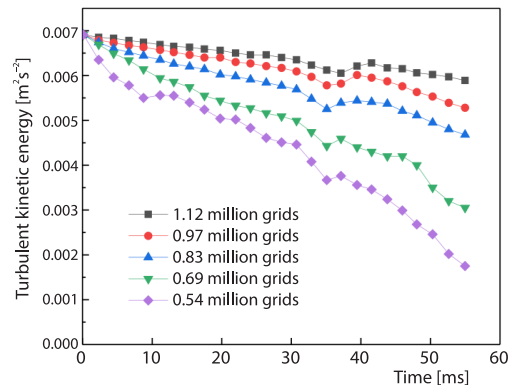


Figure 4. Grid independence verification

fluid within the water jacket. As shown in fig. 5, the maximum temperature of the permanent magnet is higher than the maximum temperature of the stator winding both before and after the adoption of the cooling pipe in the motor.

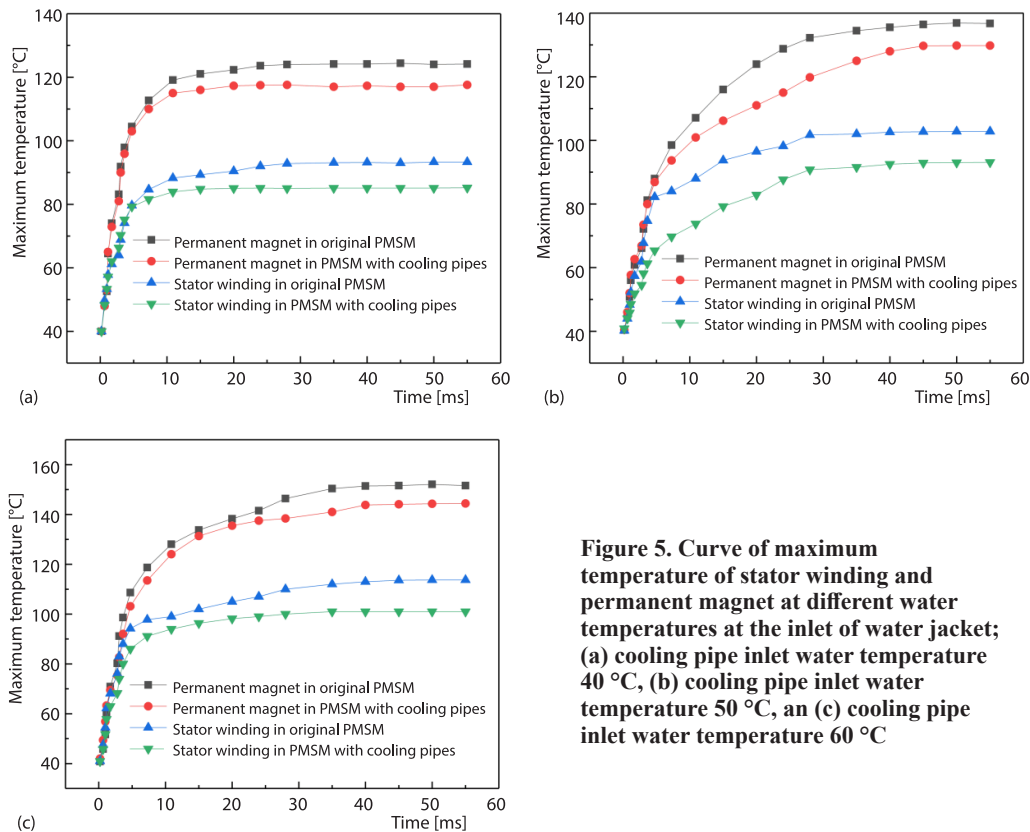


Figure 5. Curve of maximum temperature of stator winding and permanent magnet at different water temperatures at the inlet of water jacket; (a) cooling pipe inlet water temperature 40 °C, (b) cooling pipe inlet water temperature 50 °C, and (c) cooling pipe inlet water temperature 60 °C

The comparison also shows that compared with the original cooling structure, when the water temperature at the water jacket inlet is 40 °C, 50 °C, and 60 °C, respectively, the maximum temperature of permanent magnet and stator winding has decreased significantly after the motor adopts the cooling pipe. The maximum temperature of permanent magnet has decreased by 5.23%, 5.05%, and 4.69%, respectively, and the maximum temperature of stator winding has decreased by 8.68%, 9.61%, and 11.17%, respectively. From the aforementioned data it is clear that the drop in maximum stator winding temperature is greater than the drop in maximum permanent magnet temperature, this is because the cooling pipes are in direct contact with the stator core. With the increase in heat transfer area and the constant flow of cooling fluid in the cooling pipes, the heat from the stator windings is transferred to the stator core based on heat transfer. In addition, the temperature of the permanent magnets and stator windings is in a rising phase during the first 20 minutes of rated operation, after which the temperature of the permanent magnets and stator windings gradually stable.

In order to further study the temperature distribution of the stator winding of the motor with the use of cooling pipes, fig. 6 gives the specific locations of P1-P11, respectively in the stator winding, with P1-P3 and P9-P11 located in the end area of the stator winding and P4 to P8 in the slot area of the stator winding. Figure 7 shows the temperature variation curves from

P1-P11 for different water temperatures at the water jacket inlet. Figure 8 gives the temperature distribution of stator winding when water jacket inlet water temperature is 40 °C after the motor adopts cooling pipes.

According to figs. 7 and 8, after the cooling pipe is adopted for the motor, when the water jacket inlet water temperature is 40 °C, the maximum and minimum temperature of the stator winding are located at its end and the winding center, respectively. Regardless of how the cooling pipe inlet water temperature varies from 40-60 °C, the temperature distribution of the stator winding shows a strict centrosymmetric distribution, with the highest temperature of the stator winding located at P1 and P11, *i.e.* at the end of the winding, the lowest temperature of the stator winding is located at P6, *i.e.* the center of the winding. The maximum temperature difference of the stator winding is maintained at around 11 °C in all three cases with different water jacket inlet water temperatures.

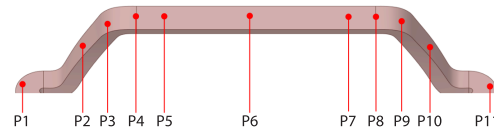


Figure 6. Specific position of P1-P11 on the stator winding

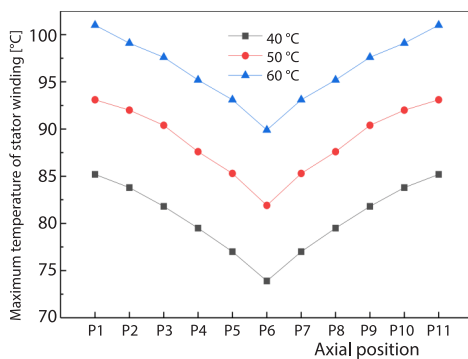


Figure 7. Curve of P1-P11 at different water temperatures at the inlet of water jacket

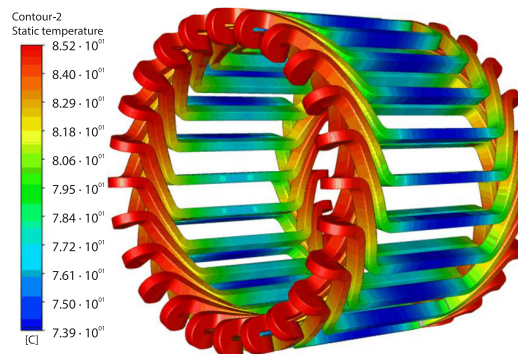


Figure 8. Temperature distribution of stator winding when the water temperature at the inlet of water jacket is 40 °C

Figure 9 gives the relationship between the maximum temperature of stator winding and permanent magnet and the water jacket inlet flow rate after the motor adopts cooling pipes. For the sake of conciseness of the figure, the following abbreviated names are marked in the upper right-hand corner of fig. 9: PM for permanent magnet, SW for stator winding, and the water temperature at the water jacket inlet is marked in brackets after PM and SW. It can be seen from fig. 9 that the maximum temperature of the stator winding and the permanent magnet does not fall at a uniform rate, when the flow rate is 1.2-2.25 m/s, the maximum temperature of the permanent magnet and the stator winding falls at a faster rate, and the maximum temperature of the stator winding generally falls at a bigger rate than the maximum temperature of the permanent magnet under the three temperature conditions, which is due to the fact that the

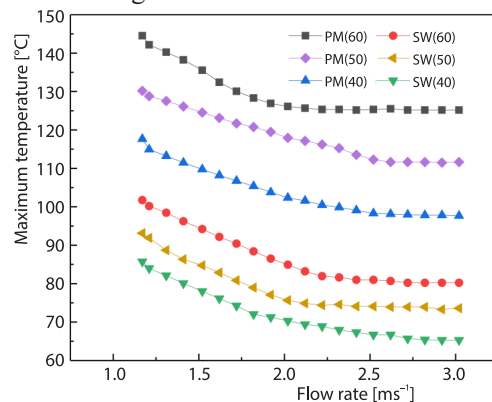


Figure 9. Curve of P-P11 at different water temperatures at the inlet of water jacket

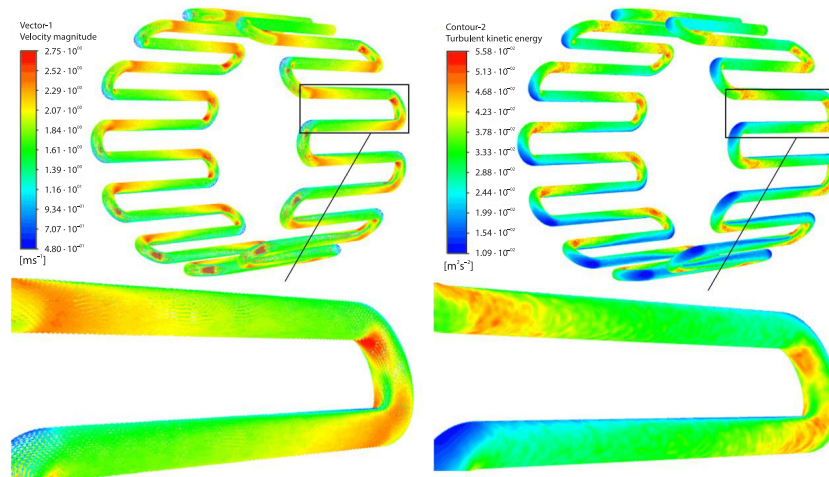


Figure 10. Velocity vector and turbulent kinetic energy distribution in cooling pipes

stator winding is spatially closer to the cooling pipes than the permanent magnet. When the flow rate is 2.25-3 m/s, the maximum temperature of the permanent magnet and stator winding gradually stabilizes.

Figure 10 shows the distribution of flow velocity and turbulent kinetic energy in the cooling pipes. As can be seen from fig. 10, the distribution of fluid velocity and turbulent kinetic energy in each cooling pipe is basically the same, both show axisymmetric distribution pattern, and the bend of the cooling pipe and the transition of the curvature of the turbulent kinetic energy are obvious energy jump, that is, the maximum turbulent kinetic energy and the minimum turbulent kinetic energy appear in the inner and outer side of the cooling pipe bend, respectively. This is due to the fact that the flow velocity decreases as the radius of curvature increases when the fluid-flows through the bend in the cooling pipes. It can also be observed visually from the fluid velocity vector diagram of the cooling pipe that the velocity decreases and then increases as the fluid-flows along the outer side of the cooling pipe, and increases and then decreases as the fluid-flows along the inner side of the cooling pipe.

Conclusions

In this paper, the 50kW PMSM for EV is taken as the research object, and the cooling pipes is used as a new water-cooled structure for the heat transfer of PMSM stator winding. The influence of the cooling pipes on the heat transfer capability of the motor is analyzed under the conditions of various temperatures and flow rates of the cooling fluid in water jacket. The main conclusions of this paper are as follows.

- Compared to the original cooling structure (water jacket), the maximum temperatures of the permanent magnets and stator windings are significantly reduced after the motor is equipped with cooling pipes, with a maximum reduction of 5.23% and 11.17%, respectively. The good heat transfer capability of the motor can be attributed to the fact that the cooling pipes directly remove the heat from the stator core by way of heat conduction, thus indirectly removing the heat from the stator windings and permanent magnets.
- The highest and lowest stator winding temperature occur at the end of the winding and at the center of the winding, respectively. The water temperature at the water jacket inlet has

no influence on the trend of the centrosymmetric temperature distribution at the center of the stator winding.

- The maximum temperature of the stator winding and the permanent magnet is not linearly related to the water jacket inlet flow rate. When the flow rate is 1.2-2.25 m/s, the maximum temperature of stator winding and permanent magnet decreases faster. When the flow rate exceeds 2.25 m/s, the maximum temperature of stator winding and permanent magnet gradually tends to be stable.
- The fluid velocity distribution in each cooling pipe is basically consistent with the turbulent kinetic energy distribution, and the maximum turbulent kinetic energy and the minimum turbulent kinetic energy occur at the inner and outer sides of the cooling pipe bend, respectively.

The new water-cooled structure proposed in this paper is still in the theoretical stage. The aforementioned research provides a reference for exploring the optimization and application of water-cooled structure of PMSM for EV from the perspective of numerical simulation. In the future, we will further study the water-cooled structure of PMSM for EV, in order to more effectively improve the heat transfer capability of PMSM.

References

- [1] Madonna, V., et al., Thermal Overload and Insulation Aging of Short Duty Cycle, Aerospace Motors, *IEEE Transactions on Industrial Electronics*, 67 (2020), 4, pp. 2618-2629
- [2] Gulec, M., et al., Magneto-Thermal Analysis of an Axial-Flux Permanent-Magnet-Assisted Eddy-Current Brake at High-Temperature Working Conditions, *IEEE Transactions on Industrial Electronics*, 68 (2021), 6, pp. 5112-5121
- [3] Du, G., et al., Power Loss and Thermal Analysis for High-Power High-Speed Permanent Magnet Machines, *IEEE Transactions on Industrial Electronics*, 67 (2020), 4, pp. 2722-2733
- [4] Sun, Y., et al., Applicability Study of the Potting Material Based Thermal Management Strategy for Permanent Magnet Synchronous Motors, *Applied Thermal Engineering*, 149 (2018), Feb., pp. 1370-1378
- [5] Huang, Z., et al., Loss Calculation and Thermal Analysis of Rotors Supported by Active Magnetic Bearings for High-Speed Permanent-Magnet Electrical Machines, *IEEE Transactions on Industrial Electronics*, 63 (2016), 4, pp. 2027-2035
- [6] Chang, J., et al., A Yokeless and Segmented Armature Axial Flux Machine with Novel Cooling System for in-Wheel Traction Applications, *IEEE Transactions on Industrial Electronics*, 68 (2021), 5, pp. 4131-4140
- [7] Vansompel, H., et al., Extended end-Winding Cooling Insert for High Power Density Electric Machines with Concentrated Windings, *IEEE Transactions on Energy Conversion*, 35 (2020), 2, pp. 948-955
- [8] Luu, P. T., et al., Electromagnetic and Thermal Analysis of Permanent-Magnet Synchronous Motors for Cooperative Robot Applications, *IEEE Transactions on Magnetics*, 56 (2020), 3, pp. 1-4
- [9] Lu, Q. F., et al., Modelling and Investigation of Thermal Characteristics of a Water-Cooled Permanent-Magnet Linear Motor, *IEEE Transactions on Industry Applications*, 51 (2015), 3, pp. 2086-2096
- [10] Dong, J., et al., Electromagnetic and Thermal Analysis of Open-Circuit Air Cooled High-Speed Permanent Magnet Machines with Gramme Ring Windings, *IEEE Transactions on Magnetics*, 50 (2014), 11, pp. 1-4
- [11] Liu, X., et al., Electromagnetic-Fluid-Thermal Field Calculation and Analysis of a Permanent Magnet Linear Motor, *Applied Thermal Engineering*, 129 (2018), Jan., pp. 802-811
- [12] Yan, W. M., et al., Electromagnetic Field Analysis and Cooling System Design for High Power Switched Reluctance Motor, *International Journal of Numerical Methods for Heat and Fluid-flow*, 29 (2019), 5, pp. 1756-1785
- [13] Zhang, B., et al., Electromagnetic-Thermal Coupling Analysis of Permanent Magnet Synchronous Machines for Electric Vehicle Applications Based on Improved ($\mu + 1$) Evolution Strategy, *IEEE Transactions on Magnetics*, 51 (2015), 4, pp. 1-10
- [14] Lindh, P., et al., Direct Liquid Cooling Method Verified with an Axial-Flux Permanent-Magnet Traction Machine Prototype, *IEEE Transactions on Industrial Electronics*, 64 (2017), 8, pp. 6086-6095

- [15] Fasquelle, A., *et al.*, Water Cold Plates Cooling in a Permanent Magnet Synchronous Motor, *IEEE Transactions on Industry Applications*, 53 (2017), 5, pp. 4406-4413
- [16] Polikarpova, M., *et al.*, Hybrid Cooling Method of Axial-Flux Permanent-Magnet Machines for Vehicle Applications. *IEEE Transactions on Industrial Electronics*, 62 (2015), 12, pp. 7382-7390
- [17] Fan, X., *et al.*, Ventilation and Thermal Improvement of Radial Forced Air-Cooled FSCW Permanent Magnet Synchronous Wind Generators, *IEEE Transactions on Industry Applications*, 53 (2017), 4, pp. 3447-3456
- [18] Sun, Y., *et al.*, Experimental and Numerical Investigation on a Novel Heat Pipe Based Cooling Strategy for Permanent Magnet Synchronous Motors, *Applied Thermal Engineering*, 170 (2020), 114970
- [19] Chen, W., *et al.*, Design and Optimization of Dual-Cycled Cooling Structure for Fully-Enclosed Permanent Magnet Motor, *Applied Thermal Engineering*, 152 (2019), Apr., pp. 338-349
- [20] Fan, X., *et al.*, Water Cold Plates for Efficient Cooling: Verified on a Permanent-Magnet Machine with Concentrated Winding, *IEEE Transactions on Industrial Electronics*, 67 (2020), 7, pp. 5325-5336
- [21] Acquaviva, A., *et al.*, Design and Verification of in-Slot Oil-Cooled Tooth Coil Winding PM Machine for Traction Application, *IEEE Transactions on Industrial Electronics*, 68 (2021), 5, pp. 3719-3727